Tellus (2000), 52B, 423–438
Printed in UK. All rights reserved

TELLUS
ISSN 0280–6509

Time-scale analysis of marine boundary layer aerosol evolution: Lagrangian case studies under clean and polluted cloudy conditions

By CLAUDIA HOELL[1], COLIN O'DOWD[1]*, SIMON OSBORNE[2] and DOUG JOHNSON[2], [1]*Centre for Marine and Atmospheric Sciences, School of Sciences, University of Sunderland, Sunderland SR2 7BW, UK;* [2]*Meteorological Research Flight, DERA, Farnborough, Hampshire, GU14 0LX, UK*

(Manuscript received 3 February 1999; in final form 20 September 1999)

ABSTRACT

Significant changes were observed in the sub-micron aerosol size distribution during a clean and a polluted Lagrangian study of marine boundary layer (MBL) aerosol and meteorological evolution during ACE-2. These changes were accompanied by significant alterations in boundary layer meteorology and structure. The clean case (LAG1) shows a reduction in the fine mode aerosol from 1050 cm^{-3} to 750 cm^{-3} and an increase in the accumulation mode concentration from 76 cm^{-3} to 162 cm^{-3} over 26 h. Dominant meteorological features during the same period comprised a reduction in boundary layer height from $\approx$1500 m to $\approx$800 m and an increase in the surface layer wind speed from 5 $m\,s^{-1}$ to 15 $m\,s^{-1}$. A detailed time-scale analysis, based upon measured data and including processes such as coagulation, condensation, deposition, chemical processing, sea-salt flux and entrainment, suggests that the dominant loss process for fine mode aerosol is coagulation, while the enhancement of accumulation mode aerosol can be almost totally ascribed to enhanced sea-salt aerosol flux into the reduced mixed layer volume. Aerosol size distributions from the polluted Lagrangian (LAG2) indicated little growth in particle diameter, and both fine and accumulation mode were observed to decrease in concentration from 2700 cm^{-3} to 1150 cm^{-3} and from 670 cm^{-3} to 430 cm^{-3} in 26 h, respectively. Dilution with cleaner free tropospheric air as the boundary layer height increased from $\approx$500 m to $>$1000 m is suggested to be the primary factor relating to reduced aerosol concentrations in this case. To a smaller extent, coagulation and precipitation scavenging were calculated to be of some importance. For both Lagrangian case studies, meteorological changes, followed by physical aerosol-cloud interactions, appear to have the greatest influence on the MBL aerosol size distribution and number concentration over the given time-scale.

1. Introduction

Atmospheric aerosols contribute to the radiative budget of the earth directly by scattering and absorbing incoming solar radiation and indirectly by influencing the microphysical, and consequently, the optical properties and the lifetime of clouds (e.g., IPCC, 1995). Alterations in number concentration, size distribution or chemical composition of the aerosol may therefore have considerable impact on the net flux of radiation through the earth's atmosphere. An important example is the interaction between aerosols and maritime stratiform clouds, which cover large areas of the ocean and whose albedo is much higher than that of the sea surface (Slingo, 1990). Because of the low susceptibility of these clouds, aerosols can

* Corresponding author. Also at: Department of Physics, University of Helsinki, PO Box 9 (Siltavuorenpenger 20D), Helsinki, FIN-00014, Finland.
e-mail: colin.odowd@cmas.demon.co.uk

have a strong effect on their properties (O'Dowd et al., 1999a; O'Dowd et al., 1999b; Durkee et al., 1999). While the aerosol influences clouds, they in turn can have an impact on aerosol physical and chemical properties. For example, Hoppel et al. (1986) and Hoppel et al. (1994) illustrated how the passage of aerosol through clouds leads to the development of a bi-modal size distribution with a fine mode (mode diameter $d \approx 30$–60 nm) and an accumulation mode ($d \approx 150$–250 nm). This process was attributed to particle growth by aqueous phase oxidation of dissolved trace gases in activated cloud droplets, especially the oxidation of SO_2 by hydrogen peroxide and ozone in cloud liquid water. O'Dowd et al. (1999c) found that, under favourable conditions, the accumulation mode aerosol gradually grew in mean diameter after successive passages through marine stratocumulus. Comparison with modelling studies showed, that the measurements could be explained by liquid-phase sulphate production in cloud.

Aerosols are also subject to several microphysical and chemical processes in the cloud-free atmosphere, influencing both particle number concentration and size distribution. Particles are removed from or added to the spectrum by dry deposition (Sievering et al., 1992), precipitation scavenging (Hoppel et al., 1994), mixing between air masses of boundary layer and tropospheric origin (Raes, 1995) or the production of sea-salt particles (O'Dowd et al., 1996). Loss and gain rates are sensitive to particle size. Mechanisms such as diffusive coagulation, self-coagulation, condensation growth and chemical processing, add mass to particles that are already part of the spectrum, thus causing a shift towards larger dry diameters.

To study the relative importance of these processes in shaping the aerosol size distribution in the marine boundary layer (MBL), airborne Lagrangian experiments were conducted during the ACE-2 field campaign (Raes et al., 2000; Verver et al., 2000) in both clean and polluted air. Johnson et al. (2000a) give a full description of the experimental design and rational of the Lagrangian studies. In summary, an air mass was tagged using an inert tracer and smart balloons released from the research ship R/V *Vodyanitsky*, and for the following 26 h, airborne measurements were conducted in the same air parcel. This allowed observations of the evolution of boundary layer thermodynamics, aerosol and cloud microphysical and chemical properties over nearly 30 h.

Before performing detailed process-model studies of the aerosol evolution during the Lagrangians, it is useful to estimate the relative importance of different mechanisms under the specific conditions present during the experiments. Calculating particle loss, production and growth rates in a time-scale analysis, based on measured MBL and aerosol features, allows the most dominant processes to be identified at an early stage. This paper presents such an analysis for the ACE-2 clean and polluted Lagrangian experiments (LAG1, LAG2). No analysis is presented for the second polluted Lagrangian experiment (LAG3), since negligible aerosol evolution was observed (Wood et al., 2000).

2. Processes and time-scale calculations

2.1. Dry deposition

Dry deposition summarises all mechanisms by which particles and gas species are removed from the atmosphere in absence of precipitation. It is mainly dominated by surface properties, turbulent features and shape, size and density of the particles. A simple approach to estimate the removal rate $(\mathrm{d}N/\mathrm{d}t)_\mathrm{D}$ of particles by dry deposition flux per unit time is (Smith et al., 1990)

$$\left(\frac{\mathrm{d}N}{\mathrm{d}t}\right)_\mathrm{D} = -v_\mathrm{d} N h_\mathrm{m}^{-1}. \tag{1}$$

All parameters influencing the removal process are included in the dry deposition velocity v_d. Values for v_d as a function of particle diameter and wind speed were derived from experimental data by Slinn et al. (1978). N is the average number concentration of particles in the mixing volume with altitude h_m. For this analysis, h_m is assumed to be the height of the well-mixed surface layer.

2.2. Precipitation scavenging

Precipitation scavenging describes the removal of particles from the atmosphere by collision with rain drops. The number removal rate of aerosol due to scavenging below precipitating clouds is

(Seinfeld and Pandis, 1997)

$$\frac{dN}{dt} = -\Lambda_n N. \quad (2)$$

For the simplified scenario of a monodisperse aerosol being scavenged by a monodisperse droplet mode, the mean number scavenging coefficient Λ_n is proportional to the collision efficiency between particles and rain drops and the drop falling velocity.

2.3. Sea-salt production

An upwards flux of sea-salt aerosol, formed by the bursting of small bubbles at the sea surface (Blanchard, 1980), is considered to enhance the concentration of sub-micrometer aerosol in the clean MBL (O'Dowd and Smith, 1993; Murphy et al., 1998). Nilsson et al. (1998) suggest a relation

$$\log\langle N'w'\rangle = ku - m,$$

between wind speed u in $m\,s^{-1}$ and the flux $\langle N'w'\rangle$ in $10^6\,m^{-2}\,s^{-1}$ of salt particles from the sea surface, where N' and w' are small-scale fluctuations in the number of particles per m^3 and the vertical wind speed component, respectively. The regression parameters k and m were derived from fits of the flux-relation to data measured by Nilsson et al. (1998). The production rate for sea-salt particles in $cm^{-3}\,s^{-1}$ is

$$\frac{dN}{dt} = 10^{ku-m}(h_{MBL})^{-1}, \quad (3)$$

where $k = 0.217$ and $m = 2.79$. Production rates and resulting increases in number concentration are calculated taking into account the evolution of the MBL height h_{MBL} and the surface layer wind speed over the observed periods.

2.4. Mixing of MBL and free tropospheric air

An increase in the MBL volume due to a rising subsidence inversion causes mixing of MBL and free tropospheric air. As particle concentrations in both air masses are usually different, the concentration in the MBL will reach a new value N_M. In a simplified approach, N_M can be determined from the mean of the initial concentrations in the MBL N and in the free troposphere N_{FT}, weighted by the original height of the MBL h_{MBL} and the increase in height Δh

$$N_M = (Nh_S + N_{FT}\Delta h)(h_S + \Delta h)^{-1}, \quad (4)$$

with $\Delta h = h_E - h_S$, h_S and h_E are heights of the subsidence inversion at begin and end of the observed period of time. This estimation assumes mixing over the whole MBL and only takes into account large-scale average changes in particle concentrations. It neglects the complex processes involved in the local entrainment process at the subsidence inversion (Nicholls and Leighton, 1986).

2.5. Coagulation

To calculate coagulation loss rates for particles, a simplified model of 2 monodisperse fractions of particles with concentrations N_1, N_2 and diameters d_1, d_2 ($d_1 < d_2$) can be applied. In this case, the coagulation rate, quantifying the reduction in N_1 due to coagulation with particles (N_2, d_2) per unit time, is (Seinfeld and Pandis, 1997):

$$\frac{dN_1}{dt} = -N_1 N_2 K_{12}, \quad (5)$$

with coagulation coefficients K_{12} as a function of d_1, d_2. Coagulation causes an increase in mass m_2 and therefore acts as a growth mechanism for particle category 2. With the mass balance

$$-\frac{dm_1}{dt} = \frac{dm_2}{dt} \approx \frac{m_2(t+\Delta t) - m_2(t)}{\Delta t},$$

$$\frac{dm_1}{dt} = \frac{1}{6}\pi d_1^3 \rho_p \frac{dN_1}{dt},$$

ρ_p referring to the particle density, the growth time $t_D = \Delta t$ for a single particle 2 from d_{21} to d_{22} is:

$$t_D = (K_{12}N_1)^{-1}\frac{d_{22}^3 - d_{21}^3}{d_1^3}, \quad (6)$$

assuming that N_1 does not change significantly during the growth process. For the following analysis, 3 types of coagulation are considered. Diffusive coagulation between particle populations **1** and **2** acts as a loss mechanism for mode **1**. Simultaneously, particles of mode **2** increase in size by taking up the mass removed from mode **1**. For example, particles with diameters just below the accumulation mode (i.e., the largest sized fine mode particles) are thus capable of growing into the accumulation mode by diffusive coagulation of smaller fine mode particles. As coagulation coefficients are strongly size dependent, the effect-

iveness of the process is significantly enhanced in cloud, where some of the particles below the accumulation mode can also be activated into cloud droplets with sizes in the μm-range. However, in the analysis reported later, we chose to examine growth of particles just above the fine-accumulation mode partition into the mid-to-higher size regimes of the accumulation mode since this growth time-scale is more rapid than for those lying below the partition.

Self-coagulation, i.e., coagulation of particles or cloud droplets within one mode ($d_1 = d_2$), is described by a slightly modified version of eq. (2) (Seinfeld and Pandis, 1997):

$$\frac{dN_1}{dt} = -0.5 N_1^2 K_{11}, \tag{7}$$

with the self-coagulation coefficient K_{11}. This study includes the following coagulation processes:

- cloud-free diffusive coagulation of the fine mode with larger aerosol modes;
- in-cloud diffusive coagulation between the fine mode and cloud droplets;
- self-coagulation within each mode (i.e., fine, accumulation and cloud droplet mode).

Coagulation with coarse mode particles ($d > 500$ nm), apart from cloud droplets, is neglected. Coalescence resulting from scavenging by large falling droplets is ignored in cloud, but is accounted for in precipitation scavenging below cloud.

2.6. Condensation growth

Oxidation of SO_2 by OH radicals leads to the formation of sulphuric acid H_2SO_4, which readily condenses on particles. Previously measured peak OH concentrations for cloud free conditions at near-similar latitudes are typically of the order of 5×10^6 molecules cm^{-3} while for cloudy conditions, there are of the order of $10^6\ cm^{-3}$ or less (O'Dowd et al., 1999d). As no measurements of OH where available for this particular experiment, a typical value for the MBL of 10^6 molecules cm^{-3} (Lin et al., 1992; Seinfeld and Pandis, 1997) is used. However, an average concentration of $10^6\ cm^{-3}$ over the duration of the experiment is very unlikely and growth time-scales derived for OH-related processes must be considered as an upper limit for the relevant rate. The net production rate for H_2SO_4 in the gas-phase is

$$\frac{d[H_2SO_4]}{dt} = k[SO_2][OH] - 2\pi d_S D[H_2SO_4]N_S \times \left(1 + \frac{8\lambda}{3\alpha d_S}\right)^{-1}. \tag{8}$$

The first term on the right-hand side describes the H_2SO_4-formation, the reaction rate k for the oxidation reaction being $k = 1.2 \times 10^{-12}\ cm^3$ per molecule and second (Atkinson et al., 1989). The second term quantifies the loss rate of H_2SO_4 to a constant surface area sink of particles with diameter d_S and concentration N_S and is taken from Schwartz (1986). Parameters are diffusion coefficient D and mean free path λ of H_2SO_4 in air and the sticking coefficient α. Under steady state conditions, i.e., $d[H_2SO_4]/dt = 0$, the concentration $[H_2SO_4]$ can be calculated after eq. (8). The condensation growth rate dd/dt of a fine mode particle can be determined by setting the loss term of eq. (8) equal to the change in particle mass, expressed as the change in dry particle diameter d_{dry}:

$$0.5\rho_{H_2SO_4} d_{dry}^2 \frac{dd}{dt} = d_{wet} D m_{H_2SO_4}[H_2SO_4]\left(1 + \frac{8\lambda}{3\alpha d_{wet}}\right)^{-1}; \tag{9}$$

$m_{H_2SO_4}$ is the mass of one molecule of H_2SO_4 and $\rho_{H_2SO_4}$ the H_2SO_4 density.

2.7. Aqueous-phase chemistry

In an aqueous solution with $pH > 3$, all SO_2 is dissolved into S(IV) species. S(IV) can be converted to S(VI) by aqueous-phase oxidation reactions, triggered mainly by H_2O_2 and O_3. When these reactions occur in deliquescent aerosols or cloud droplets, they effectively grow the particle solute mass by increasing the amount of SO_4^{2-} in the liquid/solid phase. This SO_4^{2-} contributes to the particle mass in the form of sulphuric acid or salts (Lin et al., 1992). The growth rate, derived from the mass balance between change in dry particle mass and production rate A in mol per unit volume and time of SO_4^{2-} is

$$\frac{dd}{dt} = \frac{1}{3}\frac{M_p}{\rho_p}\frac{d_{amb}^3}{d_{dry}^2} A, \tag{10}$$

where d_{amb} denotes either the ambient particle

diameter when the air parcel is out of cloud or the cloud droplet diameter when in cloud. M_p and ρ_p are molar mass and density of the substance that forms the particle. Depending on the amount of ammonia available, this will be sulphuric acid H_2SO_4, ammonium bisulphate NH_4HSO_4 or ammonium sulphate $(NH_4)_2SO_4$ (Seinfeld and Pandis, 1997). For the time-scale calculations, formation of ammonium bisulphate with $M_p = 115 \times 10^{-3}$ kg mol^{-1} and $\rho_p = 1.78 \times 10^3$ kg m^{-3} is assumed. A is given by Lin et al. (1992) as

$$A = k_6[H_2O_2][SO_2] + k_7[O_3][SO_2] \times (1 + K_4[H^+]^{-1} + K_4K_5[H^+]^{-2}),$$

with reaction rates k_i and equilibrium constants K_i for the main conversion reactions from S(IV) to S(VI). Solving eq. (10) delivers a relationship for the growth time from dry diameter d_0 to d_1:

$$t_{IC} = \rho_p(d_{amb}^3 M_p A)^{-1}(d_1^3 - d_0^3), \quad (11a)$$

for in-cloud conditions or

$$t_{CF} = \frac{3}{8}\rho_p(M_p A)^{-1} \ln\frac{d_1}{d_0} \quad (11b)$$

in a cloud-free environment ($d_{amb} = 2d_{dry}$). For these calculations, we assume that all SO_2 is dissolved into solution and that the reactions are not oxidant limited. This assumption is more likely true in cloud and provides an upper limit to the time-scale of the processes involved.

2.8. Time in cloud

Most of the aerosol processing rates are sensitive to the presence of clouds, as a higher relative humidity increases the ambient particle diameter and some of the aerosol is activated into cloud droplets. As an estimation, it can be assumed that the ratio of the time in cloud t_C to the total observation time t_t is equal to the ratio of the volume filled with cloud to the total MBL volume. t_c can then be calculated after

$$t_C = t_t + \mathrm{CCR} \times \frac{h_{MBL} - h_{CB}}{h_{MBL}}, \quad (12)$$

with h_{MBL} height of the subsidence inversion, h_{CB} height of cloud base and CCR ratio of cloud cover. As vertical velocities in cloud are usually higher than in cloud-free environment, t_c is slightly overestimated by eq. (12). To adjust for this overestimation in a crude manner, we arbitrarily chose to apply a $\approx$25% reduction to the value of t_c calculated by eq. (12) in both Lagrangian cases.

3. Case studies

The time-scale analysis case studies examine the evolution of fine and accumulation mode aerosol in the MBL during LAG1 and LAG2 over a period of approximately 26 h. Mean dry diameters for fine and accumulation mode are derived from spectra measured during the Lagrangians. In order to calculate realistic time-scales, hygroscopic growth of particles in high humidity conditions in and out of cloud must be accounted for. Out of cloud, a representative boundary layer humidity of 95% is used (Johnson et al., 2000a). Measured growth factors for sub-micrometer particles during ACE-2 were between 1.6 and 1.8 at RH = 90% (Swietlicki et al., 2000). Therefore the ambient cloud-free particle size is taken to be twice the dry diameter. In cloud, relative humidity is slightly higher than 100%, leading to activation of some particles into cloud droplets. For non-activated interstitial aerosol, maximum sizes are reached at the point of peak supersaturation in the cloud, and thereafter, as the parcel continues to rise, the particles reduce slightly in size as supersaturation decreases with height. For non-activated interstitial sulphate aerosols, O'Dowd et al. (1999e) illustrated that the typical size reached is 4$\times$ that of the particle dry size. Consequently, for treating aerosol interactions in cloud, a growth factor of 4 is assumed for interstitial particle size. All calculations are performed for "ambient" RH, i.e., with ambient or in-cloud diameters, and respective coefficients are chosen accordingly. However, in order to avoid confusion, modes will still be referred to with their dry diameters.

The following sections only give a short overview over the experiments. An explicit description of synoptic conditions and measured MBL thermodynamics and microphysics evolution during the Lagrangians, details on instrumentation and measurement techniques and the C-130 flight patterns can be found in the general Lagrangian overview paper (Johnson et al., 2000a) and the LAG1 and LAG2 overviews (Johnson et al., 2000b; Osborne et al., 2000).

3.1. LAG1 — clean marine case

3.1.1. Observations. In course of this experiment, 3 flights were carried out with the C-130 between 3 and 5 July. A 4th flight was performed by the Pelican aircraft on 5 July; however, due to tracking-balloon failure, there is some doubt as to whether or not the Pelican sampled within the tagged air parcel. Consequently, data from this platform are not used. The dominant air mass was of polar origin with hardly any passage over the continent. Broken cumulus was observed during most of LAG1 (Johnson et al., 2000a).

This study focuses on changes in aerosol number and size distribution in the surface layer over a 26-h period starting at 00:30 h on 4 July. During the first flight, Johnson et al. (2000b) report a well-mixed surface layer, topped by a de-coupled cloud layer with cloud base at an altitude of $\approx$600 m. This structure is mirrored in the number concentration of the fine mode aerosol, measured by an ultrafine Condensation Particle Counter (CPC, lower cut-off diameter 3 nm, Johnson et al., 2000b). This concentration was lower in the cloud layer than in the surface layer. The number concentration of the accumulation mode aerosol, derived from passive cavity aerosol spectrometer probe (PCASP) measurements (Osborne et al., 2000) and covering $d = 100$–500 nm, showed no dependence on altitude during the whole period of observation. With the height of the subsidence inversion steadily decreasing, the surface layer grew until the whole MBL appeared to be well-mixed.

Fig. 1 illustrates the main evolution of wind speed and MBL height during the first Lagrangian. The height of the subsidence inversion decreased from $\approx$1500 m to 800 m, causing a significant reduction of the total mixing volume. Wind speed data taken from the ECMWF model at the same time indicates changes in the surface layer wind speed from 6 m s^{-1} to 15 m s^{-1}, in close agreement with the observed wind speeds (Johnson et al., 2000a). Time in cloud was calculated after eq. (12). The evolution of the MBL height was derived from a linear interpolation to the observed changes, while cloud base was assumed to be constant at 600 m. For the first third of the experiment, peak cloud droplet concentrations encountered were of the order of 50–60 cm^{-3}, while towards the end of the experiment, peak

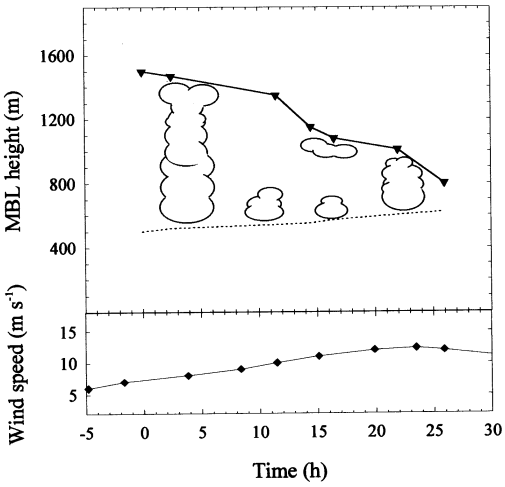

Fig. 1. Evolution of the MBL during LAG1 after Johnson et al. (2000b). Plotted are height of the subsidence inversion (triangles), height of cloud base (dotted line) and surface layer wind speed (diamonds). Wind speed is derived from the ECMWF model. Time 0 denotes the start of the period covered by the time-scale analysis.

concentrations were of ranged from 120–170 cm^{-3}. The calculations were performed with a cloud cover ratio of 3/8, which is somewhat lower than suggested by observations during the flights ($\approx$4/8), in order to account for the overestimation imposed by eq. (12). The overall time for the aerosol in cloud during the first Lagrangian is 4.6 h.

Size distributions dN/d log d of the aerosol in the surface mixed layer for start and end of the 26 h are shown in Fig. 2. The accumulation mode spectrum is derived from data of the C-130 PCASP. The fine mode spectrum is calculated from differential mobility particle sizer (DMPS) data measured on the R/V *Vodyanitskij* (Bates et al., 2000) and scaled to the total number of fine mode particles observed by the ultrafine CPC on the aircraft at start and end of LAG1, assuming the mean mode diameter of the fine mode to have remained constant over the period. This method to derive the fine mode spectrum was chosen, because no fine mode spectral data from the C-130 was available for LAG1. At the start of the experiment, the aerosol distribution was primarily bi-modal with a fine mode concentration of 1050 cm^{-3}, centred at $d_{\mathrm{dry}} = 30$ nm, and an

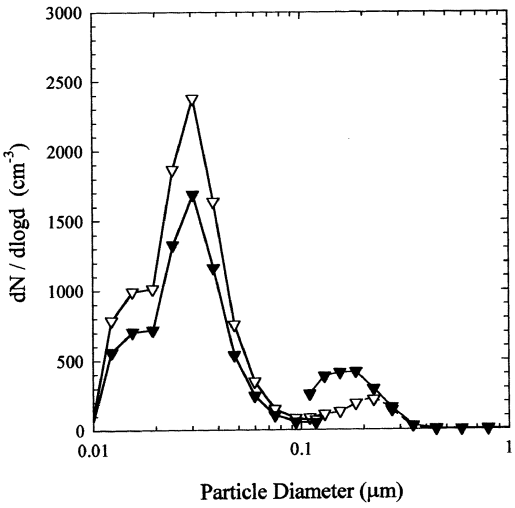

Fig. 2. Particle size distribution in the surface layer at start (open symbols) and end (filled symbols) of LAG1.

accumulation mode concentration of $76\,cm^{-3}$, centred at $d_{dry} = 220$ nm. By the end of the evolution experiment, the fine mode concentration reduced to $750\,cm^{-3}$, while the accumulation mode concentration increased to $162\,cm^{-3}$. These input values for the LAG1 case study are summarised in Table 1. The remaining fine mode particles are assumed to remain constant in size, the measured accumulation mode mean diameter however decreased to ≈ 180 nm. The observed changes suggest that (1) some of the fine mode particles grow into the accumulation mode and/or (2) there is a direct injection of new accumulation mode particles. The additional accumulation mode particles show a mode diameter smaller than the pre-existing mode.

3.1.2. Time-scale analysis. The mean wind speed in the surface layer was $8.7\,m\,s^{-1}$ for the first half of LAG1 and $12.3\,m\,s^{-1}$ for the second half. Average dry deposition fluxes calculated after eq. (1) range from $-0.44 \times 10^{-4}\,cm^{-3}\,s^{-1}$ to $-0.99 \times 10^{-4}\,cm^{-3}\,s^{-1}$ for fine mode particles and $-0.03 \times 10^{-4}\,cm^{-3}\,s^{-1}$ to $-0.04 \times 10^{-4}\,cm^{-3}\,s^{-1}$ for accumulation mode particles. Total losses over 26 h are $-6\,cm^{-3}$ particles from the fine mode and $-0.3\,cm^{-3}$ from the accumulation mode.

No precipitation was observed during the clean Lagrangian, precipitation scavenging as a loss mechanism can therefore be neglected.

The evolution of the MBL during LAG1 was dominated by a decrease in mixing volume. Therefore, mixing of MBL and tropospheric air on a large scale, as during LAG2, is unlikely to have occurred and no significant changes in MBL particle concentration due to dilution by tropospheric air are expected. Local entrainment, which took place at the subsidence inversion, is not considered here.

Sea-salt particle production is calculated after eq. (3). The production rate varies between $+0.41 \times 10^{-4}\,cm^{-3}\,s^{-1}$ and $+32 \times 10^{-4}\,cm^{-3}\,s^{-1}$ alongside with changes in both wind speed and MBL height. The net gain over 26 h is $+108\,cm^{-3}$ sea-salt particles, which are assumed to have accumulation mode sizes. This result is supported by analysis of sub-micrometer particle filter samples from the C-130, which show a significant (more than 3-fold) increase in sea-salt particle mass during the course of LAG1 (Johnson et al., 2000b), as well as by filter samples measured downwind at Hidalgo (Putaud et al., 2000).

To determine whether diffusive coagulation of fine mode particles ($d_{dry} = 30$ nm) with those at the lower end of the accumulation mode ($d_{dry} =$

Table 1. *Particle number concentrations per cm³ and dry mode diameters of fine and accumulation mode in the surface layer at start and end of LAG1 and LAG2, used as input parameters for the time-scale analysis*

LAG1 — clean case particle concentration (cm^{-3})			LAG2 — polluted case particle concentration (cm^{-3})		
	start	end		start	end
fine mode $d_{dry} = 30$ nm	1050	750	fine mode $D_{dry} = 60$ nm	2700	1150
accumulation mode $d_{dry} = 250$ nm	76	162	accumulation mode $D_{dry} = 200$ nm	670	430

200 nm) can account for the enhancement of particles at the mid-to-higher end of this mode (d_{dry} = 250 nm), we perform the calculation, using eq. (5), for a concentration in this size range of 40 cm^{-3} (i.e., about half of the total accumulation mode concentration). The coagulation coefficient for ambient cloud-free conditions is $K_{12} = 2.8 \times 10^{-8}$ cm^3 s^{-1} (Seinfeld and Pandis, 1997, for this and all other coagulation coefficients). A coagulation rate of -11×10^{-4} cm^{-3} s^{-1} leads to total losses of -104 cm^{-3} particles from the fine mode in 26 h. The time to grow a particle from dry diameter 200 nm to 250 nm after eq. (6) is 111 days. The diffusive coagulation rate is increased to approximately -33×10^{-4} cm^{-3} s^{-1} by the presence of a cloud droplet mode with d_2 = 15 μm and $N_2 = 100$ cm^{-3} (Johnson et al., 2000b) and a coagulation coefficient of $K_{12} = 3.18 \times 10^{-8}$ cm^3 s^{-1}. The total loss of fine mode particles during 4.6 h in cloud is -54 cm^{-3}. A particle with $d_{dry} = 200$ nm, activated to a 15 μm-droplet, would need approximately 97 days to grow to 250 nm according to eq. (6). The loss rate due to self-coagulation of the fine mode after eq. (7) is -5×10^{-4} cm^{-3} s^{-1}, using a K_{11} of 0.97×10^{-9} cm^3 s^{-1}. 48 cm^{-3} fine mode particles are removed in 26 h. The time to grow one particle from dry diameter 30 nm to 250 nm by self-coagulation, calculated after eq. (6), is $>10^3$ days. The self-coagulation rate for the accumulation mode ($d_{dry} = 250$ nm) under the given conditions ($K_{11} = 0.39 \times 10^{-9}$ cm^3 s^{-1}) is -1.12×10^{-6} cm^{-3} s^{-1}. This leads to a loss of one particle cm^{-3} in 26 h. For self-coagulation (coalescence) in cloud, the loss rate ($K_{11} = 3.15 \times 10^{-9}$ cm^{-3} s^{-1}) of particles is significantly less than 1 cm^{-3}.

During the clean Lagrangian, SO_2-mixing ratios between 6 and 44 ppt were measured (Johnson et al., 2000b). Using a mean value of 20 ppt and assuming a hydroxyl concentration of [OH] = 10^6 molecules per cm^3, a constant surface sink with $d_S = 250$ nm, $N_S = 50$ cm^{-3}, and an accommodation coefficient $\alpha = 1$, a steady state H_2SO_4-concentration of 5.2×10^{-2} ppt is achieved. This acid-concentration leads to a growth rate of $+7.2 \times 10^{-5}$ nm s^{-1} and a particle growth time of 35 days from diameter 30 nm to 250 nm.

Growth rates due to aqueous-phase sulphur production are calculated after eq. (10) and (11a,b). Typical concentrations of gas phase species during the clean Lagrangian were 20 ppt SO_2, 0.5 ppb H_2O_2 and 30 ppb O_3. For a cloud-free environment, a growth rate of $+10^{-9}$ nm s^{-1} and an according growth time from the fine mode to the accumulation mode of the order of 10^4 days are found. The calculations were done assuming a pH of 3, which is already very high under the given conditions (Lin et al., 1992). The growth rate in cloud is $+1.7$ nm s^{-1} for a mean cloud droplet diameter of 15 μm and a pH of 6. The resulting growth time is 35 min, which is within the time the aerosol spent in cloud during the first Lagrangian.

3.1.3. Dominating processes. Loss, gain and growth rates and changes in particle numbers for LAG1 are summarised in Table 2. The observed spectral changes can be explained by a combination of coagulation and an enhanced sea-salt flux into a reduced mixing volume. Diffusive coagulation is the dominant loss process for fine mode particles, removing 54 cm^{-3} particles in, and 104 cm^{-3} particles, out of cloud. Self-coagulation contributes with around -48 cm^{-3} particles. Together, these 3 processes are able to cover $\approx$70% of the total observed fine mode losses of -300 cm^{-3} particles. The increase in the accumulation mode by 86 cm^{-3} particles can be explained by production of sea-salt particles, which accounts for $+108$ cm^{-3} particles under the given conditions. The only growth mechanism fast enough to fit into the time-scale of the experiment is the growth of particles due to aqueous-phase chemical reactions in cloud droplets with a growth time of 35 min from the fine mode to the accumulation mode, however, time-scale analysis of this processes possesses the greatest uncertainty due to the massively non-linear nature. This processes may contribute some particles to the accumulation mode, however, under given conditions the sea-salt flux is more than sufficient to explain the obervations.

3.2. *LAG2 — polluted case*

3.2.1. Observations. The experiment included 3 flights by the C-130, carried out between 16 and 18 July. The ECMWF back trajectories show a continental air mass from the north of France. Full stratocumulus cover was present during the whole period. A description of synoptic conditions and MBL evolution can be found in Johnson et al. (2000a). Osborne et al. (2000) discuss details and

Table 2. *Results of the time-scale analysis for the clean case (LAG1). Loss and gain rates are given as maximum/minimum value over the observed period*

Process	Loss/gain rates dN/dt (1e-4 $cm^{-3} s^{-1}$)	Total contribution in 26 h (particles/cm^3)	Growth rates dd/dt (nm s^{-1})	Growth time from d_1 to d_2
Dry deposition				
fine mode	−0.99/−0.44	−6		
accumulation mode	−0.04/−0.03	−0.3		
Sea-salt production	+0.41/+32	+108		
Diffusive coagulation of the fine mode				
cloud-free	−12/−11	−104		111 days (200 to 250 nm)
in cloud	−33/−32	−54 (4.6 h in cloud)		97 days (200 to 250 nm)
Self-coagulation				
fine mode	−5.3/−4.9	−48		10^3 days (30 to 250 nm)
accumulation mode	−0.01	−1		
Condensation			+7.2e-5	35 days (30 to 250 nm)
Aqueous-phase chemistry				
cloud-free			$+10^{-9}$	$>10^4$ days
in cloud			+1.4	35 min (30 to 250 nm)

results of all measurements performed on board the C-130 during LAG2.

The time of analysis covers 26 h from 02:00 h on 17 July to 06:00 h on 18 July. The MBL was well-mixed at beginning and end of the experiment, although de-coupling occurred during daytime of 17 July. The aerosol showed some layer structure, especially a pollution layer above the subsidence inversion at the beginning of the first flight, however, the surface layer aerosol appeared mostly well-mixed (Osborne et al., 2000). Possible influences of both the de-coupling and the particle layers on the overall observed changes are excluded from this study, as their time-scales were rather short compared to the total period. Fig. 3 shows the evolution of MBL altitude and surface layer wind speed during LAG2. The height of the subsidence inversion increases from 500 m to 1100 m during the observed period. This suggests mixing of free tropospheric air into the MBL. The modelled surface layer wind speed decreases from 10 m s^{-1} to below 8 m s^{-1} during the first half of the 26 h. After that it remains rather constant

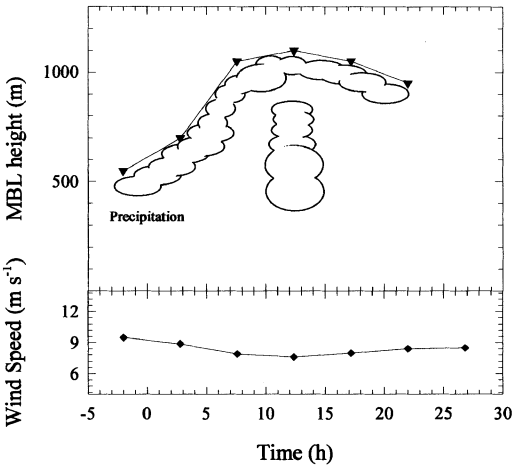

Fig. 3. Evolution of the MBL during LAG2 (Osborne et al., 2000). Shown are the height of the subsidence inversion (triangles) and the wind speed in the surface layer (diamonds), derived from the ECMWF model. Time 0 is the start of the period covered in the time-scale analysis.

between 8–9 m s^{-1}. The depth of the cloud layer was $\approx$150 m. Additionally, cumuli were observed in the middle of the observation period. Peak cloud droplet concentration approached 300 cm^{-3} for the stratocumulus cloud encountered and 400 cm^{-3} for cumulus.

An estimation of the time in cloud after eq. (12) with a constant stratocumulus depth $h_{MBL} - h_{CB} =$ 150 m and CCR = 1 results in $t_c = 4$ h, which is somewhat shorter than the 6.5 h estimated by Osborne et al. Fig. 4 shows particle size distributions $dN/d\log d$ for begin and end of the 26-h period, measured by a scanning mobility particle sizer (SMPS) and active scattering aerosol spectrometer probe (ASASP-X) on board the C-130 (Johnson et al., 2000a). The aerosol size distribution during the start of this experiment was bi-modal with a fine mode at $d_{dry} = 60$ nm, $N =$ 2700 cm^{-3} and an accumulation mode at $d_{dry} =$ 100 nm, $N = 670$ cm^{-3}. By the end of the experiment there was no change in modal diameter in either the fine or the accumulation mode, concentrations however were observed to decrease significantly in both modes. The fine mode concentration fell to 1150 cm^{-3}, the accumulation mode concentration to 430 cm^{-3}. The input parameters for the LAG2 analysis are listed in Table 3. The lack of apparent increase in mean mode diameter suggests that either no growth processes were occurring over the given time-scale or the size distribution is self-preserving in size. The loss of concentration observed in both modes suggests a significant removal processes occurring over the period.

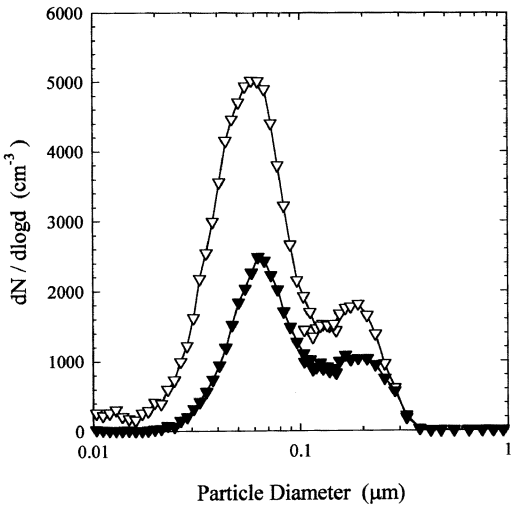

Fig. 4. Surface layer particle size distributions at start (open symbols) and end (filled symbols) of LAG2.

3.2.2. Time-scale analysis. As variations in wind speed during the polluted Lagrangian were not as large as during LAG1, dry deposition fluxes were derived for an average wind speed $u = 8.4$ m s^{-1} for the whole 26 h. Mean fluxes are between -1.45×10^{-4} cm^{-3} s^{-1} and -0.99×10^{-4} cm^{-3} s^{-1} for the fine mode and -0.51×10^{-4} cm^{-3} s^{-1} and -0.34×10^{-4} cm^{-3} s^{-1} for the accumulation mode, resulting in total losses of -11 cm^{-3} fine mode particles and -4 cm^{-3} accumulation mode particles, respectively.

Drizzle was reported during 2 flights of LAG2. Drizzle drops reached the ground only during the first observation (Osborne et al., 2000). Scavenging rates were calculated after eq. (2) for an assumed rain drop diameter $d_{drop} = 0.4$ mm. Numerically derived values for ambient Λ_n were taken from Seinfeld and Pandis (1997). They are $\Lambda_n \approx 8.3 \times 10^{-6}$ s^{-1} for scavenging of particles with $d_{dry} = 60$ nm and $\Lambda_n \approx 2.5 \times 10^{-6}$ s^{-1} for $d_{dry} = 200$ nm. Resulting scavenging rates are -224×10^{-4} cm^{-3} s^{-1} to -213×10^{-4} cm^{-3} s^{-1} for fine mode particles and $-16 - 10^{-4}$ cm^{-3} s^{-1} for accumulation mode particles. Assuming 2 h of precipitation, the total losses are -158 cm^{-3} particles from the fine mode and -12 cm^{-3} particles from the accumulation mode. These numbers agree well with results from Osborne et al., who estimate about 8% of the aerosol number is removed per day at the observed precipitation rate.

Production rates for sea-salt particles were calculated after eq. (6), using the wind speed evolution shown in Fig. 3. Values for the production rate range from $+0.63 \times 10^{-4}$ cm^{-3} s^{-1} to $+2.2 \times 10^{-4}$ cm^{-3} s^{-1}, a total of $+11$ cm^{-3} accumulation particles is gained over 26 h.

A significant increase in MBL-volume during LAG2 is indicated in Fig. 3. Particle numbers in the free troposphere were usually lower than in the MBL, except for a short interval at the beginning of the first flight, when a polluted layer was observed above the subsidence inversion. Neglecting this pollution, the mixing process induced by the change in volume had to reduce the particle concentration in the MBL. Concentrations N_M at the end of the 26-h interval are calculated after eq. (4) with an initial MBL-

Table 3. *Results of the time-scale analysis for the polluted case (LAG2). Loss and gain rates are maximum/minimum values over 26 h*

Process	Loss/gain rates dN/dt (1e-4 $cm^{-3} s^{-1}$)	Total contribution in 26 h (particles/cm^3)	Growth rates dd/dt (nm s^{-1})	Growth time from d_1 to d_2
Dry deposition				
fine mode	−1.45/−0.99	−11		
accumulation mode	−0.51/−0.34	−4		
Mixing				
fine mode		−1145		
accumulation mode		−285		
Sea-salt production	+2.2/+0.63	+11		
Precipitation				
fine mode	−224/−312	−158		
accumulation mode	−16.8/16.5	−12 (2 h precipitation)		
Diffusive coagulation of the fine mode				
cloud-free	−5.95/−5.82	−55		83 days (150 to 200 nm)
in cloud	−176/160	−241		5.7 days (150 to 200 nm)
Self-coagulation				
fine mode	−25/21	−215		227 days (60 to 200 nm)
accumulation mode	−0.90/−0.88	−8		
Condensation			+0.5e-4	35 days (60 to 200 nm)
Aqueous-phase chemistry				
cloud-free			+7.03e-6	$>10^3$ days
in cloud			+2.64	2.3 min (60 to 200 nm)

height of 500 m, a change in altitude of +600 m and free tropospheric particle concentrations of 1000 cm^{-3} in the fine mode and 200 cm^{-3} in the accumulation mode. Reductions due to the mixing are −1145 cm^{-3} fine mode particles and −285 cm^{-3} accumulation mode particles.

As in LAG1, we explore the growth time-scale for particles at the lower end of the accumulation mode sizes ($d_{dry} = 150$ nm) to grow into sizes in the mid-to-higher end of the accumulation mode ($d_{dry} = 200$nm) by diffusive coagulation with fine mode particles ($d_{dry} = 60$ nm). Since there is approximately one third of the accumulation mode particles occupying the lower size of the mode, we calculate the coagulation coefficient for a concentration of $N = 200\ cm^{-3}$ in this size range. Using a coagulation coefficient of $K_{12} = 1.1 \times 10^{-9}\ cm^3\ s^{-1}$, and taking account of the concentrations in both the fine mode and the subset of the accumulation mode, a coagulation rate of $-5.9 \times 10^{-4}\ cm^{-3}\ s^{-1}$ is derived from eq. (5), leading to a total loss of $-55\ cm^{-3}$ particles in 26 h. Eq. (6) gives a time of 83 days for a particle to grow from $d_{dry} = 150$ nm to 200 nm by this process. Coagulation with cloud droplets is calculated for a cloud droplet mode with $d_2 = 14$ μm, $N_2 = 250\ cm^{-3}$ (Osborne et al., 2000). With a coagulation coefficient $K_{12} = 2.6 \times 10^{-8}\ cm^3\ s^{-1}$, eq. (5) delivers a mean loss rate of $-167 \times 10^{-4}\ cm^{-3}\ s^{-1}$ for the fine mode. During 4 h in cloud, 241 cm^{-3} fine mode particles are thus removed. The growth time for an activated sub-

accumulation mode particle to 200 nm after eq. (6) is 5.7 days. The ambient self-coagulation coefficient for particles with $d_{dry} = 60$ nm is 6.8×10^{-10} cm^3 s^{-1}, the resulting self-coagulation rate for the fine mode after eq. (7) is -23×10^{-4} cm^{-3} s^{-1}. 215 cm^{-3} particles would therefore be removed over 26 h. Eq. (6) gives a time of 227 days to grow a particle from the fine to the accumulation mode by self-coagulation. Self-coagulation in the accumulation mode after eq. (7) delivers a loss rate of -0.88×10^{-4} cm^{-3} s^{-1} and total losses of -8 cm^{-3} particles, using a K_{11} of 4×10^{-10} cm^3 s^{-1}. As in LAG1, self-coagulation of cloud droplets leads to a loss of less than 1 cm^{-3} over the period.

SO_2-concentrations changed significantly during LAG2 (Osborne et al., 2000), with maximum values close to 800 ppt in the early hours of 17 July, which later deceased to <100 ppt. A mean SO_2-concentration of SO_2 of 125 ppt was used for the time-scale calculation. The surface sink for SO_2 was assumed to be the accumulation mode with $d_{dry} = 200$ nm and a mean concentration of 500 cm^{-3}. Applying eq. (8), 125 ppt SO_2 yield a steady-state H_2SO_4-concentration of 0.3 ppt. The resulting condensation growth rate for a particle after eq. (9) is $+0.5 \times 10^{-4}$ nm s^{-1}, the growth time from fine mode to accumulation mode 35 days. Performing the same calculation for a SO_2 mixing ratio of 750 ppt over 26 h results in a growth time of 5 days.

Growth rates and times for aqueous-phase oxidation reactions after eqs. (10) and (11a,b) are calculated for $[SO_2] = 125$ ppt, mixing ratios for O_3 and H_2O_2 are equal to LAG1. In cloud-free environment, a growth rate of $+7.0 \times 10^{-6}$ nm s^{-1} results in a growth time from fine mode to accumulation mode of 10^3 days. In cloud, assuming a fraction of particles activated to cloud droplets with diameter 14 μm, a growth rate of $+2.64$ nm s^{-1} leads to a growth time of 2.3 min.

3.2.3. Dominant processes. The results of the time-scale analysis for LAG2 are summarised in Table 3. The dominant mechanism is mixing of MBL and tropospheric air, which reduces particle concentrations in the fine mode by -1145 cm^{-3} in fine and -285 cm^{-3} in the accumulation mode. Coagulation, accounting for total losses of -511 cm^{-3}, and precipitation scavenging with losses of -158 cm^{-3}, provide additional sinks for fine mode particles. The accumulation mode concentration is reduced by -285 cm^{-3} due to the mixing. In comparison, all other processes influencing this mode, i.e., sea-salt production, are negligible. The observed reductions in number concentration of -1200 cm^{-3} in the fine mode and -240 cm^{-3} in the accumulation mode can be sufficiently explained by mixing and coagulation, although aqueous phase time-scales suggest there should be some growth from the fine mode to the accumulation mode. The net overestimation of losses may be causes by the fact that the mixing in of air from the elevated pollution layer at the beginning of the experiment, which increased the number of particles in both modes (Osborne et al., 2000), was neglected in this study. It is interesting to note that in-cloud diffusive coagulation losses for the fine mode are higher relative to diffusive coagulation out of cloud during LAG2 whereas they are lower in LAG1. This primarily results from the non-linear relationship between coagulation coefficients as a function of size. For LAG1, the difference in coagulation coefficients for the converted wet sizes in and out of cloud (60 nm and 120 nm) is significantly larger than the difference encountered in LAG2 (120 nm and 240 nm). Consequently, the smaller the fine mode is, the more likely that diffusive coagulation out of cloud will dominate over that in cloud.

4. Discussion

Fully integrated meteorological and process aerosol-cloud-chemistry models are computationally demanding. It is therefore useful to determine what processes can either be eliminated, included explicitly, or parameterised in large scale models. The purpose of this time-scale analysis is essentially to highlight, which processes should receive the greatest attention regarding inclusion of full micro-physical or chemical components. Consequently, a high degree of accuracy is not to be expected, particularly as processes are treated as individual rather than as interacting. Nevertheless, the range of errors associated with the variance in the most sensitive inputs to each calculation for the dominant processes should be examined. Four dominant processes emerge from the time-scale analysis: (1) coagulation as a loss mechanism of fine mode particles; (2) sea-salt production; (3) entrainment as an exchange

process; and (4) in-cloud chemical processing as a growth mechanism.

For the self-coagulation analysis, the most sensitive input parameter is the mode diameter used. Increasing the initial d_{dry} by 20% results in less than a 7% decrease in loss rates for both Lagrangians, while decreasing it by 20% results in a maximum of 12% over-estimate in loss rates. For diffusive coagulation out of cloud, increasing d_{dry} by 20% decreases losses by 27% in LAG1 and 2% in LAG2. Decreasing the initial size by 20% leads to an over-prediction in losses of 27% in LAG1 and 9% in LAG2. For diffusive coagulation in cloud, increasing d_{dry} by 20% decreased the losses by 4% while decreasing d_{dry} by 20% results in a 7% enhancement in calculated losses.

For the production of sea-salt, allowing a -20% error in the source rates results in a 33% reduction in the predicted sea-salt concentration, while allowing a $+20\%$ error in the source rates leads to a 74% enhancement in the predicted concentration during LAG1. For LAG2, the under-prediction is 6% while the over-prediction is 14% for the same range of error.

The treatment of entrainment rates is quite difficult and prone to error as accurate measurements of entrainment rates are difficult to achieve. In LAG1, small scale entrainment at the FT-MBL interface was neglected, while in LAG2, this entrainment was assumed to be incorporated into the rapid increase in inversion height, and minimal in terms of mixing volume exchange after the rapid increase occurs. While the latter assumption is likely to be correct for LAG2, as the rate of increase in mixing height is larger than the calculated entrainment rate (Sollazzo et al., 2000), the former assumption is unlikely to be true for LAG1, since, even though the subsidence inversion is decreasing, entrainment is still ongoing. In an attempt to examine the influence local entrainment processes for LAG1, the derived entrainment rate ($0.013\ m\ s^{-1}$) for LAG1 given by Sollazzo et al. (2000) is used to examine the effect of this exchange of FT aerosol on the MBL concentrations. Inclusion of this entrainment processes is found to result in 25% loss of fine mode particles and 15% loss of accumulation mode particles over the period. These results lead to an over-estimation of particle loss when all processes are accounted for, particularly in the fine mode, however, there is considerable error associated with the techniques used to derived entrainment rates by Sollazzo et al. (2000). Although it was assumed that the boundary layer is always well mixed, this was not always the case as for some periods during each Lagrangian, as the boundary layer was sometimes decoupled. Nevertheless, significant mixing and exchange between the surface layer and the decoupled cloud layer will most likely have occurred due to the presence of cumulus clouds. The mixing rate between the de-coupled cumulus and surface layer is obviously significantly greater (illustrated only partially by the cloud volume at any given time) than that encountered between the cumulus layer and the free troposphere. Consequently, de-coupling of the boundary layer, in the presence of significant cumulus fields, will have little impact on the general boundary layer aerosol dilution/enhancement by entrainment at the free troposphere interface.

By far the most non-linear and least suitable process for time-scale analysis, is the aqueous phase chemistry in cloud droplets. SO_2 oxidation in the aqueous phase is highly dependent on solution pH, however, this pH is not only massively variable with particle composition, it is also massively variable with particle size which can change rapidly, particularly in cloud (O'Dowd et al., 1999e). While the time-scale arguments given here suggest that particle growth can occur rapidly through SO_2 oxidation in cloud droplets, this calculation is conducted for a single particle size and using very much idealised solution chemistry. For low SO_2-concentrations, O'Dowd et al. (1999e) have shown that use of ideal chemical solution effects can overestimate the amount of oxidation occurring by more than 100% when compared to that of the robust Pitzer treatment of non-ideal solution effects. The error is even greater when mass transport limitations are ignored. Additionally, they also illustrate that, in the presence of high sea-salt and low sulphate aerosol concentrations, similar to that encountered in LAG1, as much as 90% of SO_2 oxidation occurs in droplets activated on sea-salt nuclei. The growth of sulphate aerosol from in-cloud oxidation processes is therefore a strong function of not only SO_2, O_3 and H_2O_2, but also of sea-salt aerosol concentration (O'Dowd et al., 1999b). Consequently, given the low SO_2 and high sea-salt concentrations encountered on LAG1, it is most likely that the vast majority of SO_2-sulphate

conversion occurred in sea-salt nuclei, leaving little SO_2 available for growing sulphate nuclei significantly.

In LAG2, coinciding with high wind speeds, SO_2 concentrations rapidly fell from 800 ppt to about 100 ppt at the very beginning of the experiment. Thus, it is likely that the majority of the SO_2 was depleted to sea-salt aerosols. Total sulphate production in sulphate based nuclei is independent of sulphate nuclei concentration (O'Dowd et al., 1999e) since, if the number of sulphate based droplets is increased, the solution ionic strength increases, pH reduces and the sulphate production per individual particle is also decreased. Consequently, for polluted clouds with high concentrations of sulphate based nuclei, particularly in the presence of sea-salt nuclei, any noticeable increase in sulphate particle size will be difficult to detect. Lack of growth in LAG2 suggests that chemical cloud processing during this experiment was negligible, most likely because the aerosol had reached thermodynamic and chemical equilibrium with respect to SO_2 oxidation.

Finally, we should note that we have ignored the role of organic aerosol formation in this analysis as it is unlikely to dominate the total aerosol mass when compared to the combined sea-salt and sulphate contributions. Organics are most likely to accelerate condensation growth processes, if resulting from gas-to-particle conversion processes, and be internally linked with sea-salt if mechanically produced. Putaud et al. (2000) report average sub-micron organic carbon mass contributions of 25%, relative to 56% for combined sea-salt, ammonium and sulphate, for clean marine air and 11%, relative to 74% from sea-salt, ammonium and sulphate, for polluted air. Consequently, it is unlikely that the omission of organic aerosol will significantly affect the results reported here.

5. Conclusions

During LAG1, the aerosol evolution in a clean MBL under cloudy conditions was studied. The fine mode, centred at 30 nm, was observed to decrease in concentration from 1050 cm^{-3} to 750 cm^{-3}, while the accumulation mode concentrations increased from 76 cm^{-3} to 162 cm^{-3}. Physical processes, particularly coagulation losses in the fine mode, and sea-salt production of accumulation mode particles at the ocean surface can explain the observed spectral changes. In LAG2, under polluted conditions, the fine mode with $d_{dry} = 60$ nm, decreased from 2700 cm^{-3} to 1150 cm^{-3} while the accumulation mode concentration ($d_{dry} = 200$ nm) decreased from 670 cm^{-3} to 430 cm^{-3}. No growth in either mode was observed and the reduction in concentration is explicable by dilution with cleaner, free tropospheric air as the mixing layer deepened. In both experiments, despite significant cloud cover, there was little or no evidence for chemical processing by clouds as previously observed by Hoppel et al. (1996) and O'Dowd et al. (1999c) over much shorter time-scales. This suggests that, in this case, the ability for the existing aerosol to remove trace gases was very much diminished. Meteorology and physical aerosol interactions had the greatest influence on shaping the aerosol size distribution during these studies.

6. Acknowledgements

This research is a contribution to the International Global Atmospheric Chemistry (IGAC) Core project of the International Geosphere-Biosphere Programme (IGBP) and is part of the IGAC Aerosol Characterisation Experiments (ACE). It has been supported by the European Union under contracts ENV4-CT95–0032 (ACE2 LAGRANGIAN) and ENV4-CT97–0526 (PARFORCE) and by the UK Meteorological Office under Agreement No. Met 2a/0981. The authors would also like to thank T. Bates and P. Quinn for use of the ship-borne aerosol data.

REFERENCES

Atkinson, R., Baulch, D. L., Cox, R. F., Kerr, J. A. and Troe, J. 1989. Evaluated kinetic and photochemical data for atmospheric chemistry: supplement III IUPAC subcommittee on gas kinetic data evaluation for atmospheric chemistry. *J. Phys. Chem. Ref. Data* **18**, 881–1097.

Bates, T. S., Quinn, P. K., Covert, D. S., Coffman, D. J., Johnson, J. E. and Wiedensohler, A. 2000. Aerosol

physical properties and controlling processes in the lower marine boundary layer: a comparison of submicron data from ACE-1 and ACE-2. *Tellus* **52B**, 258–272.

Blanchard, D. C. 1980. The production, concentration and vertical distribution of the sea-salt aerosol. *Annales of the New York Academy of Science* **338**, 330–347.

Durkee, P, Johnson, D. W., Ferek, R. N., Garrett, T., Hobbs, P. V., Hudson, J., Noone, K. J., Russell, L. M., Platnick, S., Taylor, J. P., O'Dowd, C. D., Hooper, W., Durkee, P., Nielson, K., Ackerman, A., Bretherton, C., Innis, G., Kogan, Y., Flagan, R., Seinfeld, J., Smith, M. H. and Hoppel, W. A. 1999. The impact of ship produced aerosols on the micro-physical characteristics of warm stratocumulus clouds: a test of Hypotheses 1.1a and 1.1b. *J. Atmos. Sci*., in press.

Hoppel, W. A., Frick, G. M. and Larson, R. E. 1986. Effect of non-precipitating clouds on the aerosol size distribution in the marine boundary layer. *Geophys. Res. Lett*. **13**, 125–128.

Hoppel, W. A., Fitzgerald, J. W., Frick, G. M. and Larson, R. E. 1990. Aerosol size distributions and optical properties found in the marine boundary layer over the Atlantic Ocean. *J. Geophys. Res.* **95**, 3659–3686.

Hoppel, W. A., Frick, G. M. and Fitzgerald, J. W. 1994. Marine boundary layer measurements of new particle formation and the effects non-precipitating clouds have on aerosol size distribution. *J. Geophys. Res.* **99**, 14,443–14,459.

IPCC, 1995. Intergovernmental Panel on Climate Change. Climate Change 1995. Cambridge University Press.

Johnson, D. W., Osborne, S. R., Wood, R., Suhre, K., Andrae, M. O., Johnson, R., Businger, S., Quinn, P. K., Bates, T., Durkee, P., Johnson, H., Russell, L. M., Noone, K., Glantz, P., Bandy, B., O'Dowd, C., Rapsomanikis, S. and Rudolph, J. 2000a. An overview of the Lagrangian experiments undertaken during the North Atlantic Regional Aerosol Characterisation Experiment (ACE-2). *Tellus* **52B**, 290–320.

Johnson, D. W., Osborne, S., Wood, R., Suhre, K., Quinn, P., Bates, T., Andreae, M., Noone, K., Glantz, P., Bandy, B., Rudolph, J. and O'Dowd, C. 2000b. Observations of the evolution of the aerosol, cloud and boundary layer characteristics during the first ACE-2 Lagrangian Experiment. *Tellus* **52B**, 348–374.

Lin, X., Chameides, W. L., Kiang, C. S., Stelton, A. W. and Berresheim, H. 1992. A model study of the formation of cloud condensation nuclei in remote marine areas. *J. Geophys. Res.* **97**, 18,161–18,171.

Murphy, D. M., Anderson, J. R., Quinn, P. K., McInnes, L. M., Brechtel, F. J., Kreidenweis, S. M., Middlebrook, A. M., Posfai, M., Thomson, D. S. and Buseck, P. R. 1998. Sea-salt particles and aerosol radiative properties in the Southern Ocean marine boundary layer. *Nature* **392**, 62–65.

Nicholls, S. and Leighton, J. R. 1986. An observational study of the structure of stratiform cloud sheets. Part I: Structure. *Q. J. Roy. Met. Soc*. **112**, 431–460.

Nilsson, E. D., Rannik, U., Swietlicki, E., Aalto, P. P., Zhou, J. and Leck, C. 1998. Turbulent aerosol number fluxes over sea and pack ice: deposition and wind driven fluxes of sub micrometer aerosol. *J. Aerosol Sci.* **29**, suppl. 1, S505–S506.

O'Dowd, C. D. and Smith, M. H. 1993. Physicochemical properties of aerosols over the northeast Atlantic: evidence for wind-speed related submicron sea-salt aerosol production. *J. Geophys. Res.* **98**, 1137–1149.

O'Dowd, C. D., Smith, M. H., Consterdine, I. E. and Lowe, J. A. 1996. Marine aerosol, sea-salt, and the marine sulphur cycle — a short review. *Atmos. Environ.* **31**, 73–80, 1997.

O'Dowd, C. D., Lowe, J., Smith, M. H. and Kaye, A. D. 1999a. The relative importance of sea-salt and nss-sulphate aerosol to the marine CCN population: an improved multi-component aerosol-droplet parameterisation. *Q. J. Roy. Met. Soc*. **125**, 1295–1313.

O'Dowd, C. D., Lowe, J. A. and Smith, M. H. 1999b. Coupling sea-salt and sulphate interactions and its impact on predicting cloud droplet concentrations. *Geophys. Res. Lett*. **26**, 1311–1314.

O'Dowd, C. D., Lowe, J. A. and Smith, M. H. 1999c. Observations and modelling of aerosol growth in marine stratocumulus — case study. *Atmos. Environ.* **33**, 3053–3062.

O'Dowd, C., McFiggans, G., Creasey, D. J., Pirjola, L, Hoell, C., Smith, M. H., Allan, B. J., Plane, J. M. C., Heard, D. E., Lee, J. D., Pilling, M. J. and Kulmala, M. 1999d. On the photochemical production of new particles in the coastal boundary layer. *Geophys. Res. Lett*. **26**, 1707–1710.

O'Dowd, C. D., Lowe, J. A., Clegg, N., Clegg, S. L. and Smith, M. H. 1999e. Modelling heterogeneous sulphate production in maritime stratiform clouds. *J. Geophys. Res*., in press.

Osborne, S. R., Johnson, D. W., Wood, R., Bandy, B. J., Andrae, M. O., O'Dowd, C. D., Glantz, P. and Noone, K. 2000. Observations of the evolution of the aerosol, cloud and boundary layer dynamic and thermodynamic characteristics during the second Lagrangian experiment of ACE-2. *Tellus* **52B**, 375–400.

Putaud, J. P., Van Dingenen, R., Mangoni, M., Virkkula, A.,. Raes, F., Maring, H., Prospero, J. M., Swietlicki, E., Berg, O. H., Hillamo, R. and Makela, T. 2000. Chemical mass closure and origin assessment of the submicron aerosol in the marine boundary layer and the free troposphere at Tenerife during ACE-2. *Tellus* **52B**, 141–168.

Raes, F. 1995. Entrainment of free tropospheric aerosols as a regulating mechanism for cloud condensation nuclei in the remote marine boundary layer. *J. Geophys. Res.* **100**, 2893–2903.

Raes, F., Bates, T. S., McGovern, F. M. and Van Liedekerke, M. 2000. The second Aerosol Characterisation

Experiment (ACE-2): general overview and main results. *Tellus* **52B**, 111–126.

Schwartz, S. E. 1986. Mass transport considerations pertinent to aqueous-phase reactions of gases in liquid-water clouds. In: *Chemistry of multiphase atmospheric systems* (ed. Jaeschke, W.). Springer Verlag, Berlin, 415–471.

Seinfeld, J. H. and Pandis, S. N. 1997. *Atmospheric chemistry and physics*. John Wiley & Sons, New York.

Sievering, H., Boatman, J., Galloway, J., Keene, W., Kim, Y., Luria, M. and Ray, J. 1992. Removal of sulphur from the marine boundary layer by ozone oxidation in sea-salt aerosols. *Nature* **360**, 571–573.

Slinn, W. G. N., Hasse, L., Hicks, B. B., Hogan, A. W., Lai, D., Liss, P. S., Munnich, K. O., Sehmel, G. A. and Vittori, O. 1978. Some aspects of the transfer of atmospheric trace constituents past the air-sea interface. *Atmos. Environ.* **12**, 2055–2087.

Slingo, A. 1990. Sensitivity of the Earth's radiation budget to changes in low clouds. *Nature* **343**, 49–51.

Smith, M. H., Park, P. M. and Consterdine, I. E. 1990. North Atlantic aerosol remote concentrations measured at a Hebridean coastal site. *Atmos. Environ.* **25A**, 547–555.

Sollazzo, M. J, Russell, L. M., Percival, D., Osborne, S., Wood, R. and Johnson, D. W. 2000. Entrainment rates during ACE-2 Lagrangian experiments calculated from aircraft measurements. *Tellus* **52B**, 335–347.

Swietlicki, E., Zhou, J., Covert, D. S., Hameri, K., Busch, B., Vakeva, M., Dusek, U., Berg, O. H., Wiedensohler, A., Aalto, P., Makela, J., Marinsson, B. G., Papaspiropoulos, G., Mentes, B., Frank, G. and Stratmann, F. 2000. Hygroscopic properties of aerosol particles in the north-eastern Atlantic during ACE-2. *Tellus* **52B**, 201–227.

Verver, G., Raes, F., Vogelezang, D. and Johnson, D. 2000. The second Aerosol Characterization Experiment (ACE-2): meteorological and chemical context. *Tellus* **52B**, 126–140.

Wood, R., Johnson, D., Osborne, S., Bandy, B., Andreae, M., O'Dowd, C., Glantz, P. and Noone, K. 2000. Boundary layer, aerosol and chemical evolution during the third Lagrangian experiment of ACE-2. *Tellus* **52B**, 401–422.